# Identification of Night-Time F- Region Currents from CHAMP Satellite Observations over Equatorial Africa

**Adero Awuor Ochieng*[1], Paul Baki[1], Peter Kotze[2] and Collins Mito[3]**

[1]Department of Technical and Applied Physics, Technical University of Kenya, P.O Box 52428-00200, Nairobi, Kenya
[2]South Africa National Space Agency (SANSA), P.O Box 32, Hermanus 7200, South Africa
[3]Department of Physics, University of Nairobi, P. O. Box 30197, Nairobi, Kenya

Email: aderoconstant@gmail.com

## ABSTRACT

The F-region currents are generally weak and difficult to detect. However, their contributions to the earth's magnetic field variations are significant and cannot be ignored by the field modelers. CHAMP satellite has therefore provided a perfect opportunity to investigate the in-situ F-region currents on the night side of the equatorial region. The magnitudes of the current along all the three components of the earth's magnetic field (X, Y, Z) are investigated. However in this paper, we present only the results on the Y-component where interesting magnetic residuals were observed. The X and Z-components were rather masked in much noise and would require further filtering. The currents appear in both the pre-midnight and post-midnight sectors and are spatially confined to the equatorial region bounded by the Appleton anomaly. The magnetic residuals are generally observed in the northern hemisphere of an order of 0.8nT, which gives a height-integrated current density of about 1.3mA/m.

## INTRODUCTION

The ionosphere is the part of the Earth's upper atmosphere where the ions and electrons are present in quantities sufficient to affect the propagation of radio waves (Campbell, 2003). It results when the solar radiation (Extreme Ultraviolet and X-rays) from the Sun ionizes the otherwise neutral upper atmosphere. The presence of the charged particles in the upper atmosphere makes it an electric conductor and thus supports the ionospheric currents. For purposes of investigating these electric currents, the ionosphere can be divided into two layers: the E-region lies between an altitude of about 90km to 160km, and the F-region is above it (S Maus & Lühr, 2006). The F-region contains an extensive amount of ionization that persists into the night-time, thus controlling the night-time ionospheric F-region dynamo (Rishbeth, 1971). Although, the E-region, due to recombination processes, loses the control of the ionosphere at night, it is effective during the day through the E-region dynamo. The ionosphere hosts three types of conductivities namely: direct conductivity, Hall conductivity and Pedersen conductivity (M. C. Kelley, 2009). Of these three, Pedersen conductivity becomes the most important at night. It depends on the product of ionization and collision frequency and

varies considerably with both altitude and zonal wind component. Basically the ability of the ionospheric F-region to carry currents depends on the small ratio of E to F-region height-integrated Pedersen conductivity (Lühr, Maus, Rother, & Cooke, 2002). The F-region electric currents are generally weak and difficult to detect as they are masked by a number of background perturbations. Even though the F-region has been extensively studied, only a few of these studies have focused on the night side and particularly on the Equatorial ionosphere over Africa. Currents associated with local plasma depletions using CHAMP observations were investigated by (Lühr et al., 2002) and the first observational evidence of the force of gravity as an important driver of ionospheric currents was pointed out by (Lühr, Maus, & Rother, 2004). The three major ionospheric current drivers, gravity, plasma pressure gradient and F-region dynamo, had been reported by (M. C. Kelley, 2009). The study though treated all the three components independently it did indicate that all the components contribute to the total current. In this paper we present the results from an investigation of night-time F-region currents as inferred from in situ CHAMP measurements of the vector magnetic field:-, using exclusively the magnetic Y-east pointing component. The

magnetic vector can be expressed as Cartesian components to any three orthogonal axes. The geo-magnetic elements are taken to be components parallel to the geomagnetic north and east directions and the vertically downward direction as shown in figure 1 below.
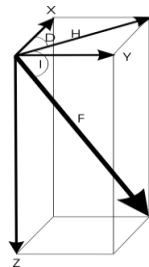


**Figure.1** Cartesian components of the geomagnetic elements, x-North, East (M. Kelley), z-vertically downward.

### OBSERVATIONS

The Challenging Mini-satellite Payload (CHAMP) was launched on $15^{th}$ July, 2000 with an initial altitude of 450km into an almost circular, near-polar orbit with an inclination of $87.3^{0}$. The primary objectives were to carry out in situ measurements related to the gravity field, the atmosphere and the magnetic field [http://op.gfz-potsdam.de/champ]. Magnetic field measurements by the fluxgate magnetometer from CHAMP satellite were used in this study. The vector data was selected from $1^{st}$ January, 2001 to $31^{st}$ December, 2001. The latitudinal consideration ranging from $-30^{0}$S to $30^{0}$N geomagnetic coordinates. The data in the North-East-Center (NEC) coordinate system were selected from the CDF files and converted into ASCII format columns in terms of year, month, day, latitude, and longitude, altitude, X, Y and Z components. Only nighttime data (20h00 to 05h00 UT) c were selected to avoid the effects of the E-region. We only considered measurements during quiet time periods with Dst $\leq$20. Magnetic field signatures recorded by CHAMP comprise the sum of contributions from various sources such as magnetic fields due to: primary contributions of the Earth's core and crust, ionosphere, magnetosphere, the magnetosphere-ionosphere coupling currents, as well as the

fields due to the coupling between hemispheres. The major contributing magnetic fields were calculated using various FORTRAN based software and field models (IGRF10, Crustal field model, cubic spline fit). The International Geomagnetic Reference Field (IGRF10) model (Stefan Maus & MacMillan, 2005) was used (spherical degree of 13) to subtract the Earth's main field contributions and the crustal field model of degree up to 90 to determine lithospheric effects. Finally to remove ring currents effects, we performed a cubic spline fit to the X, Y, and Z residuals as a function of latitude, and subtracted it from the residuals obtained from the previous data processing steps, thus leaving the external field effects resulting from F-region currents.

### RESULTS AND DISSCUSSION

The following figures show typical examples of the magnetic signatures of equatorial spread F, using the magnetic Y-component as observed by the CHAMP satellite. The phenomenon is predominant in the pre-midnight sector as depicted by (figures; 1a, 2a, 4a, 4b, 4d, 4e, 5a, 5b, 5c, 5d, 5e, 7a, 7b, and 7c). This is observed in all seasons, though most prevalent in equinox. The post-midnight signatures are also observed in all the seasons (figures 2c, 2d, 2e, 3a, 3b, 3c, 3d, 8a, 8b and 9a.), except in the summer solstice. The northern hemisphere experienced more magnetic signatures than the southern hemisphere, where only three cases were identified, figures; 3c, 6a and 6b. A peculiar feature was observed (figure 2b) where the magnetic signatures appear on both sides of the region bounded by the Appleton anomaly. The signatures are almost symmetrical at latitude $-28^{0}$, longitude $-10.28^{0}$ and latitude $28^{0}$, longitude $-11.04^{0}$. These signatures occur just after sunset, which is 20LT. The signatures mostly occur in post sunset period between 20LT-22LT. The signatures are prevalent on the east of meridian as summarized in table 1 below. There is no significant difference in the residual magnitude over the longitudinal range. However, higher values of the residuals were recorded on longitudes; $35.56^{0}$, $39.47^{0}$ and $39.52^{0}$ on the west of meridian
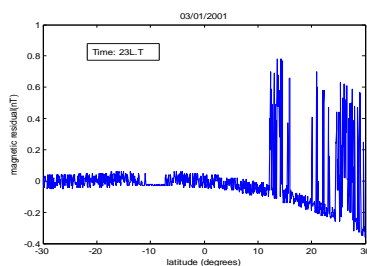


**Figure.1a** The magnetic residual is seen on various latitudes; $11^{0}, 21^{0}$ and $29^{0}$
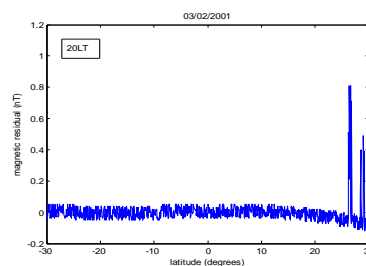


**Figure. 2a** The magnetic signature is on the northern hemisphere on an latitude $28^{0}$.
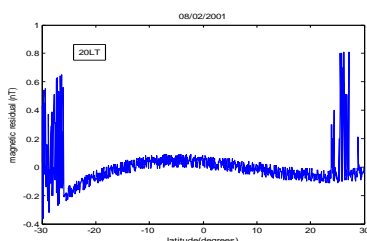


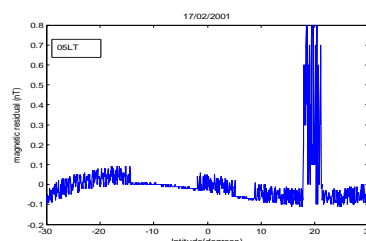**Figure.2b** A near symmetry in the magnetic signature observed.
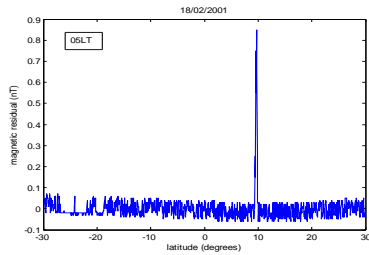


**Figure.2c** Magnetic residual is observed on latitude $20^{0}$.

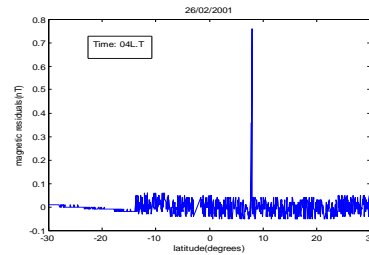**Figure.2d** A post midnight residual is observed on latitude $10^0$.



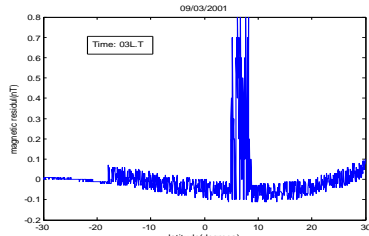**Figure.2e** A distinctive feature is observed on latitude $9^0$.



**Figure.3a** A magnetic residual of order 0.8nT is recorded on latitude $9^0$.



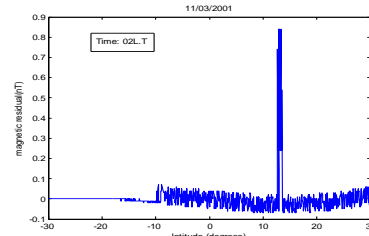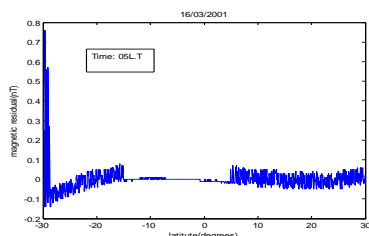**Figure.3b** A magnetic residual occurs on latitude $12^0$.



**Figure.3c** The magnetic residual is observed on the southern hemisphere latitude $-30^0$.
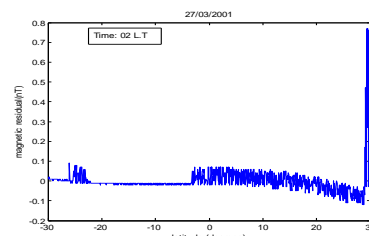


**Figure.3d** A magnetic residual is recorded on the northern hemisphere on latitude $30^0$.
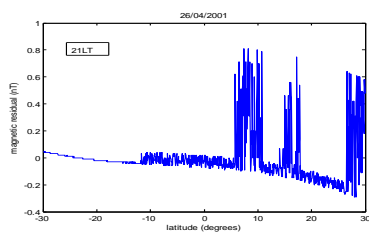


**Figure.4a** The magnetic residuals on different latitudes ($9^0, 15^0,$ and $29^0$) in the northern hemisphere.
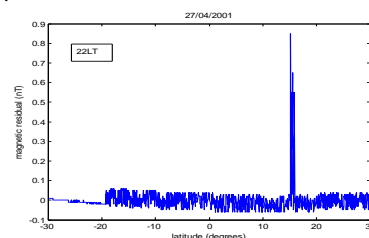


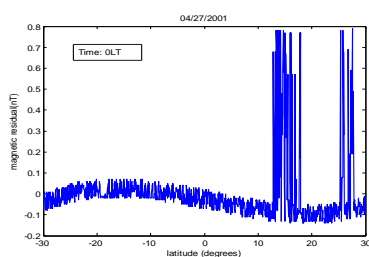**Figure.4b** The signature is observed on latitude $15^0$.



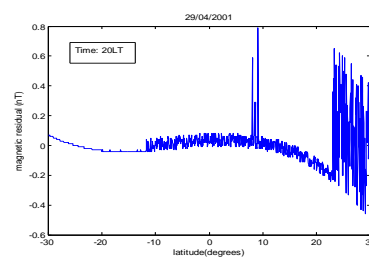**Figure.4c** Two magnetic signatures are recorded at two different latitudes $15^0$ and $28^0$.



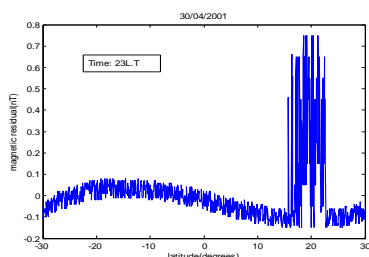**Figure.4d** Two signatures are observed on latitudes $10^0$ and $28^0$.



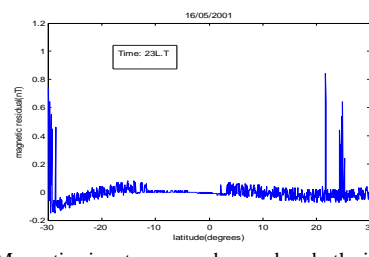**Figure.4e** The signature is observed on latitude $20^0$.



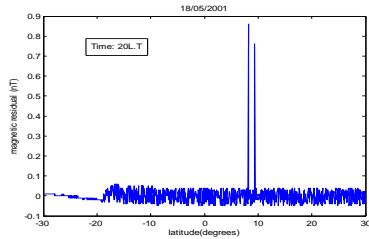**Figure.5a** Magnetic signatures are observed on both sides of the hemispheres, latitudes: $-30^0, 21^0$.
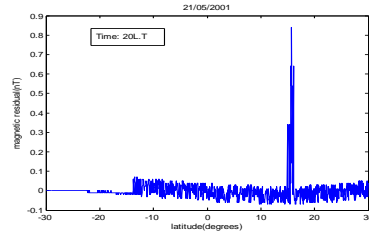
**Figure.5b** The signature is observed on latitude $9^0$.



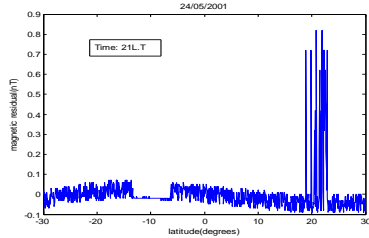**Figure 5c**. The signature is observed on latitude $15^0$.



**Figure 5d**. The magnetic signature is observed on latitude $20^0$.
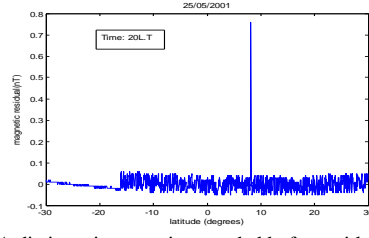


**Figure 5e**. A distinct signature is recorded before midnight on latitude $9^0$.
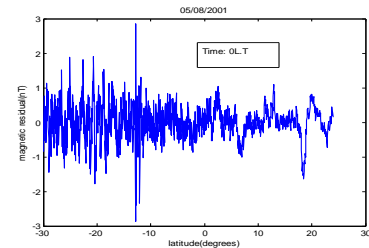


**Figure 6a**. The signature is observed on latitude $-12^0$.
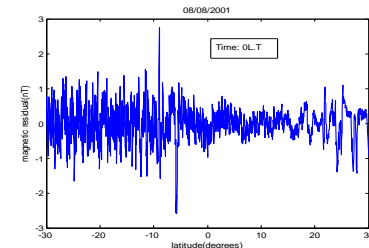


**Figure 6b**. A magnetic signatue of $\pm 2.8$nT on latitude $-7^0$ and $-10^0$.
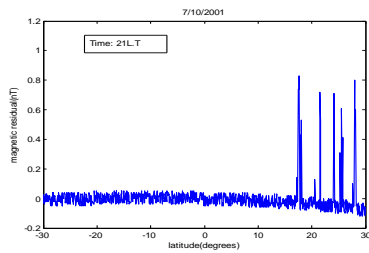


**Figure 7a**. Magnetic residuals on various latitudes; $19^0$, $25^0$, $28^0$.



**Figure 7b**. The signatures are observed on various latitudes; $9^0$, $13^0$, $25^0$ and $29^0$.



**Figure 7c**. Two magnetic residuals are observed on latitudes $10^0$ and $26^0$.



**Figure 8a**. Two signatures are seen on latitudes; $0^0$ and $15^0$.



**Figure 8b**. A magnetic signature is observed on latitude $15^0$.



**Figure 9a**. Shows a magnetic residual on latitude $20^0$

**Table.1** variation of current density with seasons, latitude, longitude and local time

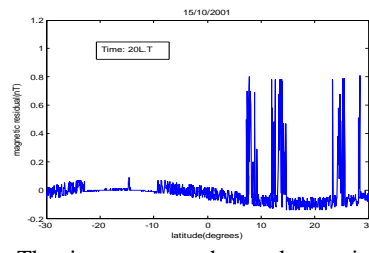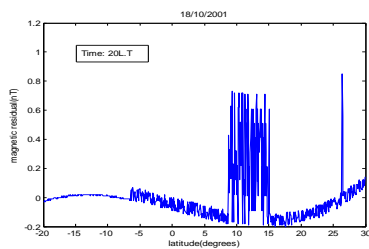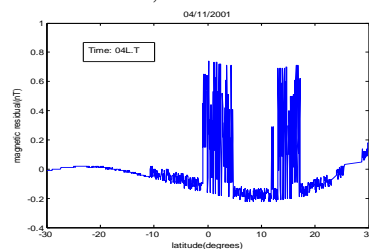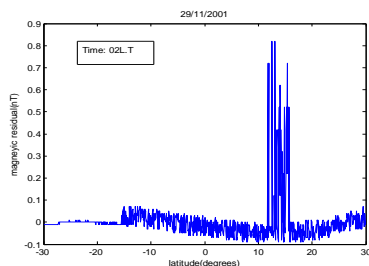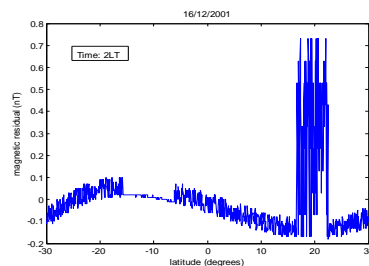| Seasons | Date | Latitude (deg) [0] | Longitude (deg) [0] | Local time | Magnetic residual(nT) | Current density (mA/m) |
|---|---|---|---|---|---|---|
| **Equinox: March** | 09/3/2001 | 9 | 19.35 | 03 | 0.8 | 1.3 |
| | 11/3/2001 | 12 | 36.35 | 02 | 0.8 | 1.3 |
| | 16/3/2001 | -30 | -15.39 | 05 | 0.78 | 1.2 |
| | 27/3/2001 | 30 | 9.15 | 02 | 0.78 | 1.2 |
| **April** | 26/4/2001 | 9 | 44.97 | 21 | 0.85 | 1.4 |
| | | 15 | 45.07 | 21 | 0.85 | 1.4 |
| | | 29 | 45.20 | 21 | 0.7 | 1.1 |
| | 27/4/2001 | 15 | 30.47 | 22 | 0.88 | 1.5 |
| | 27/4/2001 | 15 | -1.76 | 00 | 0.78 | 1.2 |
| | | 28 | -1.63 | 00 | 0.78 | 1.2 |
| | 29/4/2001 | 10 | 48.04 | 20 | 0.8 | 1.3 |
| | | 28 | 48.24 | 20 | 0.7 | 1.1 |
| | 30/042001 | 20 | 10.18 | 23 | 0.78 | 1.2 |
| **October** | 07/10/2001 | 19 | -3 | 21 | 1 | 1.6 |
| | | 25 | -3.05 | 21 | 0.9 | 1.43 |
| | | 28 | -3.07 | 21 | 1 | 1.6 |
| | 15/10/2001 | 9 | 3.16 | 20 | 0.9 | 1.43 |
| | | 13 | 3.10 | 20 | 0.9 | 1.43 |
| | | 25 | 2.97 | 20 | 0.9 | 1.43 |
| | | 29 | 2.96 | 20 | 0.9 | 1.43 |
| | 18/10/2001 | 10 | 8.45 | 20 | 0.8 | 1.3 |
| | | 26 | 8.47 | 20 | 0.9 | 1.43 |
| **Winter Solstice November** | 04/11/2001 | 0 | 37.37 | 04 | 0.8 | 1.3 |
| | | 15 | 37.61 | 04 | 0.9 | 1.43 |
| | 29/11/2001 | 15 | 26.8 | 02 | 0.85 | 1.3 |
| **December** | 16/12/2001 | 20 | 10.35 | 02 | 0.75 | 1.2 |
| **January** | 03/01/2001 | 11 | -5 | 23 | 0.8 | 1.3 |
| | | 21 | -6 | 23 | 0.8 | 1.3 |
| | | 29 | -7 | 23 | 0.8 | 1.3 |
| **February** | 08/02/2001 | -28 | -10.28 | 20 | 0.7 | 1.1 |
| | | 28 | -11.04 | 20 | 0.85 | 1.3 |
| | 17/02/2001 | 20 | 14.28 | 05 | 0.8 | 1.3 |
| | 18/02/2001 | 10 | 22.57 | 05 | 0.85 | 1.3 |
| | 26/02/2001 | 9 | 19.82 | 04 | 0.78 | 1.3 |
| **Summer solstice May** | 16/05/2001 | -30 | -12.47 | 23 | 0.7 | 1.1 |
| | | 21 | -11.75 | 23 | 0.85 | 1.3 |
| | | 25 | -11.75 | 23 | 0.7 | 1.1 |
| | 18/05/2001 | 9 | 29.25 | 20 | 0.88 | 1.4 |
| | 21/05/2001 | 15 | 32.65 | 20 | 0.85 | 1.3 |
| | 24/05/2001 | 20 | 12.64 | 21 | 0.85 | 1.3 |
| | 25/05/2001 | 9 | 21.42 | 20 | 0.75 | 1.2 |
| **August** | 05/08/2001 | -12 | 35.56 | 00 | ±3 | ±4.8 |
| | 08/08/2001 | -7 | 39.47 | 00 | ±2.8 | ±4.5 |
| | | -10 | 39.52 | 00 | ±2.8 | ±4.5 |

## IONOSPHERIC F-REGION CURRENTS

The detected night-time field perturbations in the pre-midnight and post-midnight local times can now be interpreted as caused by F-region currents. The dominant ionospheric F-region current components are the F-region dynamo, Earth's gravity field and ionospheric plasma-pressure gradient. Putting all these effects together, the resulting current density **j** is (M. Kelley, 1989)

$$j = \sigma E + \{nm_i g \times B - k\nabla[(T_i + T_e)n] \times B\}\frac{1}{B^2} \quad (1)$$

where $\sigma$ is the conductivity tensor, **E** is the electric field, $n$ is the electron density, $m_i$ the ion mass, **g** is the gravitational acceleration, $k$ is the Boltzmann constant, $T_e$ and $T_i$ are the electron and ion temperatures, and **B** is the ambient magnetic field of magnitude $B$. The first term on the right-hand side of equation (1) represents the currents due to F-region dynamo, the second the gravity driven currents and the third term plasma driven currents. The currents driven by the F-region dynamo can be derived directly from CHAMP magnetic field measurements. From peak-to-peak variation of the magnetic $B_y$ component, when passing over the equator, we can deduce the integrated, vertical current strength, $j_z$. For a crude estimate of current density we may use the infinite current sheet approximation (Lühr et al., 2002)

$$\Delta B = \frac{\mu_0}{2}j_z, \quad (2)$$

where $j_z$ is the current density, $\mu_0$ is the susceptibility of free space and $\Delta B$ the magnetic signal resulting from a current that flows in the z-direction. From our results, the peak-to-peak deflections are generally less than 1nT except for summer solstice (August, fig. 6a and 6b) where we get a magnetic residual of over $\pm 2.5$nT corresponding to height-integrated current density of over $\pm 4.5$ mA/m according to equation (2). The observed Y magnetic residuals generally have a positive sign which corresponds to a northward pointing magnetic field. These imply westward currents flowing below the satellite orbit. The pronounced residuals in the local time period 2000-2400 could be attributed to the super rotation of the low-latitude thermosphere that results in a net east-west average zonal flow of about 150m/s around 440km altitude. The solar heating of the thermosphere can also explain the high winds experienced in the post-sunset period. A near symmetry characterized by (fig.2b), where magnetic signatures appear on both sides of the equator bounded by the Appleton anomaly can be attributed to the fountain effect at the equator. The pre-reversal enhancement of the zonal wind can also be attributed to the observed post sunset residuals. The effect of this phenomenon is large eastward electric fields which are significant in the F-region where the recombination is slow. The equatorial F -region rises in height accompanied by steepening of electron density gradients on its underside following sunset, due to chemical recombination and electrodynamics effects associated with the enhancement of the eastward electric field. This leads to steep plasma density gradients on the bottom side unstable to collisional Rayleigh-Taylor (R-T)instability (Sastri, 1984).

## CONCLUSIONS

Our results compare favorably with that of the first in-situ observations of night-time F-region currents utilizing data from the CHAMP satellite. We find a spatial confinement of the currents to the near equatorial region bounded by the Appleton anomaly in both pre-midnight and post-midnight sectors (Lühr et al., 2002; Stolle, Lühr, Rother, & Balasis, 2006). Even though the zonal wind speed is known to decay in the post-midnight sector, our results are not in any way affected and more investigations need to be done. The study on the F-region currents is a precursor to the understanding of the plasma depletions, ionospheric scintillations, pre-reversal enhancements etc and therefore still needs much investigation. The X and Z-components of the field, which were masked in noise, need lots of filtering to completely determine the residuals. Comparisons of this work with ground based observations are pending. The average current density using the Y-component is generally less than 4.8mA/m

## REFERENCES

Campbell, W. H. (2003). *Introduction to geomagnetic fields*: Cambridge University Press.

Kelley, M. (1989). The Earth's Ionosphere: Plasma Physics and Electrodynamics, Int. *Geophys. Ser, 43*, 437-455.

Kelley, M. C. (2009). *The Earth's ionosphere: plasma physics and electrodynamics* (Vol. 96): Academic Press.

Lühr, H., Maus, S., & Rother, M. (2004). Noon-time equatorial electrojet: Its spatial features as determined by the CHAMP satellite. *Journal of geophysical research, 109*(A1), A01306.

Lühr, H., Maus, S., Rother, M., & Cooke, D. (2002). First in-situ observation of night-time F region currents with the CHAMP satellite. *Geophysical research letters, 29*(10), 1489.

Maus, S., & Lühr, H. (2006). A gravity-driven electric current in the Earth's ionosphere identified in CHAMP satellite magnetic measurements. *Geophysical research letters, 33*(2), L02812.

Maus, S., & MacMillan, S. (2005). 10th generation international geomagnetic reference field. *Eos, Transactions American Geophysical Union, 86*(16), 159.

Rishbeth, H. (1971). Polarization fields produced by winds in the equatorial< i> F</i>-region. *Planetary and Space Science, 19*(3), 357-369.

Sastri, J. (1984). *Duration of equatorial spread-F*. Paper presented at the Annales Geophysicae.

Stolle, C., Lühr, H., Rother, M., & Balasis, G. (2006). Magnetic signatures of equatorial spread F as observed by the CHAMP satellite. *Journal of geophysical research, 111*(A2), A02304.